CrossMark

RESEARCH PAPER

A hypoplastic constitutive model for debris materials

Xiaogang Guo[1] · Chong Peng[1] · Wei Wu[1] · Yongqi Wang[2]

Abstract Debris flow is a very common and destructive natural hazard in mountainous regions. Pore water pressure is the major triggering factor in the initiation of debris flow. Excessive pore water pressure is also observed during the runout and deposition of debris flow. Debris materials are normally treated as solid particle–viscous fluid mixture in the constitutive modeling. A suitable constitutive model which can capture the solid-like and fluid-like behavior of solid–fluid mixture should have the capability to describe the developing of pore water pressure (or effective stresses) in the initiation stage and determine the residual effective stresses exactly. In this paper, a constitutive model of debris materials is developed based on a framework where a static portion for the frictional behavior and a dynamic portion for the viscous behavior are combined. The frictional behavior is described by a hypoplastic model with critical state for granular materials. The model performance is demonstrated by simulating undrained simple shear tests of saturated sand, which are particularly relevant for the initiation of debris flows. The partial and full liquefaction of saturated granular material under undrained condition is reproduced by the hypoplastic model. The viscous behavior is described by the tensor form of a modified Bagnold's theory for solid–fluid suspension, in which the drag force of the interstitial fluid and the particle collisions are considered. The complete model by combining the static and dynamic parts is used to simulate two annular shear tests. The predicted residual strength in the quasi-static stage combined with the stresses in the flowing stage agrees well with the experimental data. The non-quadratic dependence between the stresses and the shear rate in the slow shear stage for the relatively dense specimens is captured.

Keywords Constitutive modeling · Debris flows · Granular-fluid flows · Hypoplastic model

1 Introduction

Debris flow is a very common natural hazard in the mountainous areas of many countries. It represents the gravity-driven flow of a mixture of various sizes of sediment, water and air, down a steep slope, often initiated by heavy rainfall and landslides [17]. The highest velocity of debris flows can be more than 30 m/s; however, typical velocities are less than 10 m/s [24]. The fast debris flows may cause significant erosion, while increasing the sediment charge and destructive potential. Such mass flows cause serious casualties and property losses in many countries around the world. The initiation mechanisms of debris flow and the predicted possible velocity are essential information for the design of protective measures. Numerical analysis plays an important role to obtain this information, where a competent constitutive model for debris materials is required. The main factors influencing the initiation of debris flow are, among others, the topography, material parameters, water and the initial stress state in the affected slope [22]. Earth slopes with inclinations ranging from 26° to 45° have been generally identified as most prone to debris flow initiation [40]. The common solid

✉ Wei Wu
   wei.wu@boku.ac.at

[1] Institut für Geotechnik, Universität für Bodenkultur, Feistmantelstrasse 4, 1180 Vienna, Austria

[2] Fachgebiet für Strömungsdynamik FB Maschinenbau, Technische Universität Darmstadt, Otto-Berndt-Strasse 2, 64287 Darmstadt, Germany

volume fraction of debris materials, defined as the ratio between the solid volume and the total volume of a representative volume element, varies between about 30 and 65 %. The water from heavy rainfall or snow melting makes the unconsolidated superficial deposit on a steep hillside saturated, thereby leading to a reduced shear strength due to the decreasing of matric suction, and further triggering a landslide. Such an upland landslide may develop into a hillside debris flow when the water in the sliding mass cannot be discharged quickly and therefore gives rise to excessive pore water pressure. In this case, based on the principles of soil mechanics, the effective stresses between solid particles will decrease to cause the reduction or complete loss of shear strength. Upon initiation of debris flow, debris material shows fluid-like behavior. As concluded by Iverson [19], debris flow can be mobilized by three processes: (i) widespread Coulomb failure along a rupture surface within a saturated soil or sediment mass, (ii) partial or complete liquefaction of a sliding mass due to high pore-fluid pressure and (iii) conversion of landslide translational energy to internal vibrational energy. In these processes, the development of high pore water pressure is likely the most significant triggering factor. In addition, experimental observation [18] shows that an almost constant excess pore water pressure persists during the runout and depositing of debris flows. Thus, a suitable constitutive model which can capture the solid-like behavior before failure and the fluid-like behavior after failure should has the capability to describe the developing of pore water pressure (or effective stresses) in the initiation stage and determine the residual effective stresses exactly. Some important material parameters such as solid volume fraction (or void ratio in soil mechanics) and the internal friction coefficient need to be taken into account. Actually, debris materials are normally simplified as solid spherical particle–viscous fluid mixture and treated as a fluid continuum with microstructural effect in the constitutive modeling [10, 11]. In most conventional models, constitutive equations for the static and dynamic regimes are formulated and applied separately, such as the models for the solid-like behaviors of granular materials [8, 27, 41, 43] and that for the fluid-like behaviors [1, 6, 21]. Although some models for granular-fluid flows have taken the stress state of the quasi-static stage into account, the employed theories for the static regime, such as Mohr–Coulomb criterion [34] and extended von Mises yield criterion [32], still fail to determine the changing of pore water pressure from the deformation directly. Hypoplasticity was proposed as an alternative to plasticity for the description of solid-like behavior of granular materials [41, 43]. The distinctive features of hypoplasticity are its simple formulation and capacity to capture some salient features of granular materials, such as non-linearity, dilatancy and yielding [42].

It may be the suitable choice for the description of solid-like behavior of debris materials.

In this paper, a framework which consists of a static portion for the frictional behavior and a dynamic portion for the viscous behavior is introduced at first. Bagnold's constitutive model for a gravity-free suspension [1] is chosen as the dynamic portion in the framework. Then, the applicability of a specific hypoplastic model in the description of granular-fluid flows is studied by using this model to simulate the undrained simple shear test of saturated granular materials as shown in Fig. 1, which is in analogy to the initiation of a debris flow. The dynamic model, which is modified by fitting Bagnold's experimental data and taking a parameter termed critical solid volume fraction into account [15], is combined with the hypoplastic portion to obtain a new complete constitutive model for debris flows. The performance of the proposed model is demonstrated by some element tests in which the new model is used to simulate two annular shear tests with different materials and apparatus.

2 The framework of constitutive modeling for debris materials

As stated in the preceding section, debris materials show solid-like behavior before failure and fluid-like behavior after failure. This particular phenomenon cannot be modeled only within the framework of statics or dynamics. An applicable model may need to combine a static and a dynamic portion and make the transition from solid-like to fluid-like behavior turns out as an outcome [42].

In our former work [15], based on the velocity analysis of dry sand flow [4, 26] and the force balance of an inclined plane supporting a uniform layer of sand–water mixture beneath a uniform layer of pure water [34], a framework for the constitutive model of debris materials was developed as the following form,
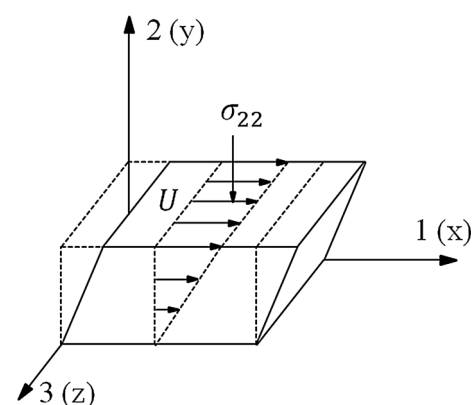

Fig. 1 Schematic of undrained simple shear tests

$$P = P_0 + P_i \tag{1a}$$

$$T = T_0 + T_v + T_i, \tag{1b}$$

where P and T are the normal and shear stresses for the solid phase; P_0 and T_0 are the normal and shear stress caused by prolonged contact between particles; T_v, T_i and P_i are slightly modified Bagnold's constitutive relations for a gravity-free dispersion of solid spheres sheared in Newtonian liquids. The stresses P_0 and T_0 are the static portion of the framework which satisfy a generalized Mohr–Coulomb type yield criterion [9, 31]. Thus,

$$T_0 = P_0 \tan\phi \tag{2}$$

where ϕ denotes the residual friction angle after failure. They correspond to the residual stresses of debris materials in the quasi-static stage. For a simple shearing, the shear stress for the so-called macro-viscous regime, T_v, has the following expression

$$T_v = K_1 \frac{dU}{dy} \tag{3}$$

where the coefficient K_1 is related to the material property and expressed as

$$K_1 = \left[(1+\lambda)\left(1 + \frac{1}{2}\lambda\right) - \frac{1}{1+\lambda} \right]\left(1 - \frac{C}{C_c}\right)^{-n} \mu; \tag{4}$$

U is the shear velocity as shown in Fig. 1 and dU/dy denotes the shear rate changing along the depth direction; C is the mean solid volume fraction and C_c is the maximum solid volume fraction to assure a full shearing to occur; n is a fitting parameter and μ is the dynamic viscosity of the interstitial fluid; λ is a dimensionless parameter termed linear concentration. For perfectly spherical particles, λ is defined as

$$\lambda = \frac{d}{s} = \left[\left(\frac{C_\infty}{C}\right)^{\frac{1}{3}} - 1 \right]^{-1} \tag{5}$$

where s is the mean free distance between two particles; C_∞ is the asymptotic limit of the maximum measured solid volume fraction as the container dimensions approach infinity, which is also related to the size of the particles [16]. The shear stress for the 'grain-inertia' regime, T_i, is formulated as

$$T_i = K_2 \left(\frac{dU}{dy}\right)^2 \tag{6}$$

in which

$$K_2 = 0.042 R_v \rho_s (\lambda d)^2 \sin\alpha_i \tag{7}$$

is also a coefficient related to the material property and

$$R_v = \frac{K_1}{2.25\lambda^{\frac{3}{2}}\mu} \tag{8}$$

is a correction factor based on the experimental results in [1]; ρ_s and d denote the material density and mean diameter of the grains, respectively; the tangent of the angle α_i corresponds to the ratio between the shear and normal stress in the 'grain-inertia' regime. Therefore, the expression of the normal stress in the 'grain-inertia' regime is

$$P_i = \frac{T_i}{\tan\alpha_i} = \frac{K_2}{\tan\alpha_i}\left(\frac{dU}{dy}\right)^2. \tag{9}$$

T_v, T_i and P_i are termed the dynamic portion of the framework (1). This framework implies that the contributions of contact friction, fluid viscosity and particle collisions coexist in the entire flow process. Bagnold's tests [1] for two different interstitial fluids with different viscosities but the same density show significant differences in the slow shear stage and tend to the same stress–strain relation when the shear velocity is large enough. In the rapid shear stage, the particle collisions become very fierce; the bulk behavior and dissipation of the flow kinetic energy are dominated by the inelastic and frictional particle collisions. An impact between two particles in a viscous liquid approximates a dry impact since the fluid effect is insignificant in comparison with the collision force in this stage [45]. Therefore, the linear term T_v, rather than the quadratic terms T_i and P_i, makes the models based on the framework (1) capable of distinguishing granular-fluid mixtures with different interstitial fluid. The dry granular flow can be treated as a particular case where air is the interstitial fluid.

For a free surface dry granular flow shown in Fig. 2, the viscous terms T_v are normally much less than the residual strength T_0 in the beginning of the flow since the shear rate is very small in this stage. It is also negligible in the fast shearing stage since the viscous effect of air is insignificant compared to the frictional and collisional effect of particles.
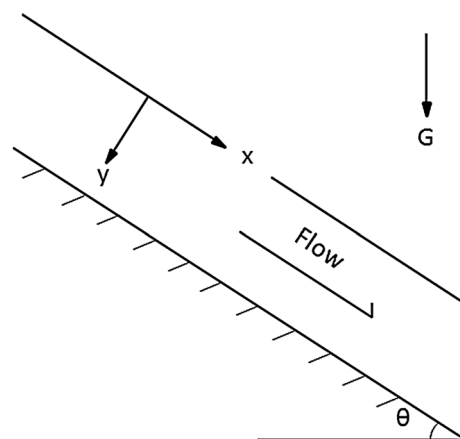

Fig. 2 Schematic of an uniform granular-fluid flow on a slope

Thus, the framework (1) will be reduced to the following form in the case of free surface dry granular flow.

$$P = P_0 + P_i \qquad (10a)$$

$$T = T_0 + T_i. \qquad (10b)$$

As stated in the literature [26], the relation (6) predicts a steady uniform flow only when the slope θ is equal to the angle α_i. However, experimental results [3] show that such steady flow can be obtained not only at a single slope but over a slope range. This experimental observation can be predicted by the reduced framework (10) [25, 31]. According to force balance when a steady uniform flow is obtained in the free surface dry granular flow, we have

$$P_0 + P_i = \rho_s C g h \cos\theta \qquad (11a)$$

$$P_0\tan\phi + P_i\tan\alpha_i = \rho_s C g h \sin\theta \qquad (11b)$$

where g is the gravity acceleration; h is the depth along the y axis which is normal to the flow bed. Then we get the stress ratio

$$\frac{P_0\tan\phi + P_i\tan\alpha_i}{P_0 + P_i} = \tan\theta. \qquad (12)$$

Let us assume that α_i is greater than the residual friction angle ϕ, which is consistent with the experimental observations of dry granular flows [30]. The normal stress P_i is zero in the critical state of triggering the flow since the flow velocity is almost null at that time point. Thus, from (11) and (12), we obtain

$$P_0 = \rho_s C g h \cos\theta_1 \qquad (13)$$

and

$$\tan\theta_1 = \tan\phi \qquad (14)$$

where θ_1 is the critical inclination for the granular material start flowing. With the increasing of inclination, another critical state will be reached. In this state, the component of gravity perpendicular to the flowing bed is totally supported by P_i since the flow velocity is large enough at this inclination. From (12), we get

$$\tan\theta_2 = \tan\alpha_i \qquad (15)$$

where θ_2 is the maximum inclination for equation (12) holds. It indicates that the framework (10), in which the stresses are divided into a static portion generated by prolonged contact of particles and a dynamic portion produced in particle collisions, can predict steady uniform flows over a slope range $\theta \in [\phi, \alpha_i]$. By taking the effect of the interstitial fluid into account, a constitutive model developed within the complete framework (1) can describe not only dry granular flows but also granular-fluid flows.

In the above analysis, the simple formula for the initial value of P_0, (13), is only applicable for free surface dry

granular flows. As pointed out in the preceding section, debris materials are saturated solid–fluid mixtures which will be partially or fully liquefied in the initiation of debris flows. The normal stress P_0 is the effective stress and obtained by subtracting the excess pore water pressure from the total normal stress in this case. A proper theory is required to capture the partial or complete liquefaction, and further determine the residual strength P_0 and T_0. As introduced before, hypoplasticity may be the suitable choice for the description of solid-like behavior of debris materials. In the following section, we study the capability of a specific hypoplastic model for capturing the main properties of debris materials in the quasi-static stage.

3 The applicability of hypoplastic models for debris materials

Hypoplastic constitutive equations are based on nonlinear tensorial functions with the major advantages of simple formulation and few parameters. Two hypoplastic models, the one developed by Wu et al. [41] and the one by Gudehus [13], are compared in the selection of the static portion for the framework (1). In the more recent models by Gudehus [13], mainly the stiffness is modified by the two factors, f_b and f_e, which take into account the influence of stress state and density, respectively. In modeling debris flow, however, the strength is very important and the stiffness is not important. Moreover, his model makes use of the exponential functions for the dependence of critical void ratio and minimum void ratio on pressure. For each function the parameters reduce from 3 to 2. However, there are only few data in the literature for the exponential functions. Therefore, in this paper, we will embark on the model proposed by Wu et al. [41] which is the first hypoplastic model with critical state to verify that, by employing an appropriate hypoplastic model as the static portion, the combined model based on the framework (1) can fulfill an entire and quantitative description of stress state for debris materials from quasi-static stage to fast flow stage.

It is worth mentioning that the hypoplastic model with critical state is just one of the choices for describing the initiation of debris flows. Recently some improved models have been available, e.g. [12, 23, 35], which are developed from some widely used versions of hypoplastic model [28, 37] and aim to improve the dependence of stiffness on pressure and density. However, the capability of these models for capturing the phenomenon of liquefaction and the stability in the cases of large deformation or low confining pressure still need to be verified. A more concise hypoplastic model with the former mentioned capability and stability can be employed to determine the stress state in the quasi-static stage of debris materials.

The hypoplastic model with critical state is an improvement of a basic hypoplastic model for sand developed by Wu and Bauer [43] as

$$\mathring{\mathbf{T}}_h = c_1(\mathrm{tr}\mathbf{T}_h)\mathbf{D} + c_2 \frac{\mathrm{tr}(\mathbf{T}_h\mathbf{D})\mathbf{T}_h}{\mathrm{tr}\mathbf{T}_h} + \left(c_3 \frac{\mathbf{T}_h^2}{\mathrm{tr}\mathbf{T}_h} + c_4 \frac{\mathbf{T}_h^{*2}}{\mathrm{tr}\mathbf{T}_h}\right) \parallel \mathbf{D} \parallel \quad (16)$$

where $c_i(i = 1, \ldots, 4)$ are dimensionless material parameters; $\mathbf{T}_h$ and $\mathbf{D}$ denote the stress tensor and the strain rate tensor, respectively; $\mathbf{T}_h{}^*$ is the deviatoric stress tensor expressed by

$$\mathbf{T}_h{}^* = \mathbf{T}_h - \frac{1}{3}(\mathrm{tr}\mathbf{T}_h)\mathbf{1}; \quad (17)$$

$\parallel \mathbf{D} \parallel = \sqrt{\mathrm{tr}(\mathbf{D}^2)}$ stands for the Euclidean norm and $\mathbf{1}$ is unit tensor. The Jaumann stress rate tensor $\mathring{\mathbf{T}}_h$ in (16) is defined by

$$\mathring{\mathbf{T}}_h = \dot{\mathbf{T}}_h + \mathbf{T}_h\mathbf{W} - \mathbf{W}\mathbf{T}_h \quad (18)$$

where $\dot{\mathbf{T}}_h$ is the stress rate tensor (material time derivative of $\mathbf{T}_h$); $\mathbf{W}$ denotes the spin tensor. The hypoplastic model (16) possesses simple mathematical formulation and contains only four material parameters, $c_1 \sim c_4$. The specific determination process of $c_1 \sim c_4$ can be obtained in the literatures [5, 41, 43]. Two stress states, the initial hydrostatic and the state at failure, are chosen for the identification of $c_1 \sim c_4$ based on a triaxial test with constant confining pressure, i. e. $\dot{\mathbf{T}}_h(2,2) = \dot{\mathbf{T}}_h(3,3) = 0$. And then, the following parameters are introduced:

the stress ratio, $R = \mathbf{T}_h(1,1)/\mathbf{T}_h(3,3)$;

the initial tangent modulus,

$$E_i = [(\dot{\mathbf{T}}_h(1,1) - \dot{\mathbf{T}}_h(3,3))/\mathbf{D}(1,1)]_{R=1};$$

the initial Poisson ratio, $v_i = [\mathbf{D}(3,3)/\mathbf{D}(1,1)]_{R=1}$;

the failure stress ratio, $R_f = [\mathbf{T}_h(1,1)/\mathbf{T}_h(3,3)]_{\max}$;

the failure Poisson ratio, $v_f = [\mathbf{D}(3,3)/\mathbf{D}(1,1)]_{R=R_f}$.

The failure stress ratio R_f and the failure Poisson ratio v_f are related to the friction angle ϕ_0 and the dilatancy angle ψ, respectively, through the following relations [43]:

$$R_f = \frac{1 + \sin\phi_0}{1 - \sin\phi_0} \quad (19)$$

and

$$v_f = \frac{1 + \tan\psi}{2}. \quad (20)$$

Taking the four material constants $c_1 \sim c_4$ as unknowns, a system of four linear equations can be obtained by substituting the corresponded stress and strain rate of the two stress states into the model (16). Therefore, the material constants are determined as functions of the well-established parameters in soil mechanics, the initial tangent modulus E_i, the initial Poisson ratio v_i, the friction angle ϕ_0 and the dilatancy angle ψ. It should be pointed out that these parameters are related to a specific confining pressure, all the sets of material constants used in this paper are obtained with a confining pressure $\mathbf{T}_h(3,3) = 100\,\mathrm{kPa}$. In addition, the deviatoric loading in the initial hydrostatic state is considered to be zero, i. e. the initial Poisson ratio $v_i = 0$.

By taking the effect of void ratio and stress level into account, the model (16) was slightly modified to the following form [41].

$$\mathring{\mathbf{T}}_h = c_1(\mathrm{tr}\mathbf{T}_h)\mathbf{D} + c_2 \frac{\mathrm{tr}(\mathbf{T}_h\mathbf{D})\mathbf{T}_h}{\mathrm{tr}\mathbf{T}_h} + \left(c_3 \frac{\mathbf{T}_h^2}{\mathrm{tr}\mathbf{T}_h} + c_4 \frac{\mathbf{T}_h^{*2}}{\mathrm{tr}\mathbf{T}_h}\right) \parallel \mathbf{D} \parallel I_e, \quad (21)$$

where

$$I_e = (a - 1)D_c + 1 \quad (22)$$

is a factor called density function. a is a material parameter related to the stress level and

$$D_c = \frac{e_{\mathrm{crt}} - e}{e_{\mathrm{crt}} - e_{\min}} \quad (23)$$

is the modified relative density; e is the void ratio; $e_{\min}$ and e_{crt} are the minimum and the critical void ratio, respectively. The effect of void ratio and stress level on the behavior of granular materials is taken into account in the model (21) by using the following expressions,

$$e_{\mathrm{crt}} = p_1 + p_2\exp(p_3 \mid \mathrm{tr}\mathbf{T}_h \mid), \quad (24)$$

and

$$a = q_1 + q_2\exp(q_3 \mid \mathrm{tr}\mathbf{T}_h \mid) \quad (25)$$

where $p_i(i = 1, \ldots, 3)$ and $q_i(i = 1, \ldots, 3)$ are material parameters and can be determined by fitting the experimental data of drained triaxial tests under different confining pressure; $\mid \cdot \mid$ denotes absolute value. It is shown that the model (21) is applicable to both initially and fully developed plastic deformation of granular materials with drained or undrained conditions [41, 43]. It will reduce to the original one (16) when the void ratio e is equal to the critical value e_{crt} from (22) and (23). It means, for same material, same constants $c_1 \sim c_4$ will be obtained for the original and extended models in the case of $e = e_{\mathrm{ecrt}}$. Thus, the material constants emerging in the model (21) can be determined by the same way as done for (16). The dilatancy angle ψ is equal to zero since there is no volume

deformation in this case [44]. About the material parameters $p_i(i = 1, ..., 3)$ and $q_i(i = 1, ..., 3)$, some theoretical and experimental analyses are presented in [41]. p_1 is the critical void ratio when the confining pressure approaches infinity, since p_3 is negative. The value of p_1 should be close to the minimum void ratio under a high confining pressure. For the case of zero confining pressure, the critical void ratio is equal to $p_1 + p_2$ which may close to the maximum void ration measured with very low confining pressure. q_1 is assumed to be always equal to 1 and q_3 is a negative value. For the case of $\mathrm{tr}\mathbf{T}_h \to \infty$, the difference between dense and loose packing tends to disappear since the parameter $a \to 1$. Based on the numerical parametric study [41], q_2 is suggested to lie in the range $(-0.3, 0.0)$. p_3 and q_3 for quartz sand are assumed to be -0.0001 kPa. In the case of very low confining pressure, such as the state of liquefaction, relatively higher values of q_2, p_3 and q_3 may be needed to keep the sensitivity of I_e to the stress level.

The hypoplastic model (21) may be a proper choice for describing the shear softening (liquefaction) and the residual strength in the beginning of a debris flow. During debris flow, the material is subjected to large shear deformation. For developing and evaluating constitutive models, the planar simple shear motion is particularly relevant [14]. Therefore, we try to verify the applicability of the hypoplastic model (21) in the simulation of debris flows initiation by using this model to reproduce the typical experimental results of granular materials in undrained simple shear tests. As presented in the literatures [7, 46], saturated sand specimens with different initial void ratios demonstrate three types of stress–strain behavior in undrained simple shear tests as indicated in Fig. 3: (i) the dense specimens have tendency of dilation and show shear hardening to reach a ultimate steady state (USS) finally; (ii) the very loose specimens demonstrate shear softening to obtain constant residual strength or complete liquefaction in the critical steady state (CSS); (iii) the specimens with medium void ratio first soften, then harden and reach also a ultimate steady state [47]. The shear softening is considered to be the main mechanism in the mobilization of debris flows.

Now we intend to reproduce these three types of stress–strain behavior in the element tests. The experimental results will be reproduced qualitatively rather than precisely, due to some important material parameters are not presented in the literature [46]. In order to obtain the material constants $c_1 \sim c_4$ for sand in the critical state with $I_e = 1$, the initial tangent modulus E_i is determined approximately by the following relation [20, 36]

$$\frac{E_i}{P_a} = 150 \left(\frac{\sigma_{33}}{P_a}\right)^{0.5}, \tag{26}$$
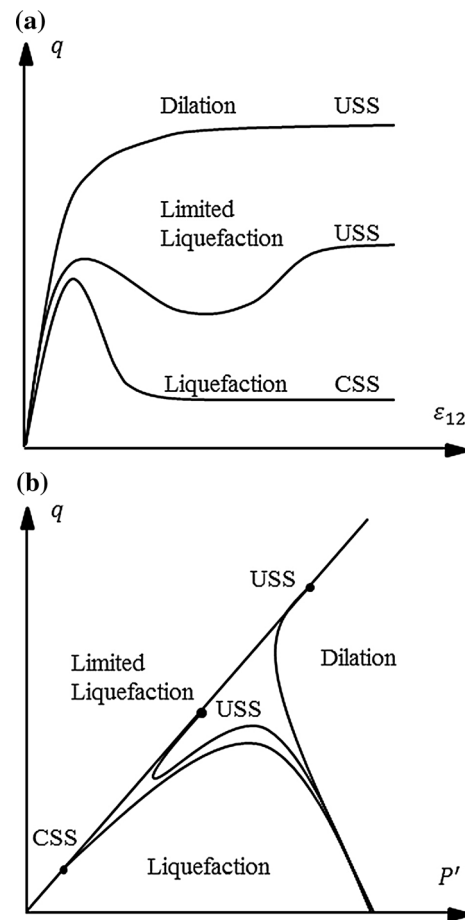

Fig. 3 Three types of stress–strain behavior observed in undrained triaxial tests and undrained simple shear tests: **a** shear strain versus shear stress, **b** mean principal stress versus shear stress

in which P_a is the atmospheric pressure (101.3 kPa) and σ_{33} is the effective confining stress, given as 100 kPa in the experiments. Thus, the initial tangent modulus is obtained approximately 15 MPa. The friction angle ϕ_0 is assumed equal to a relatively small value, 25°, for saturated loose sand in the critical state with $e = e_{\mathrm{crt}}$. Both the initial Poisson ratio υ_i and the dilatancy angle ψ are assumed to be 0 as stated before. The determined material constants for the model (21) are presented in Table 1.

The three types of stress–strain behavior are reproduced as shown in Fig. 4, when the values in Table 2 are employed for p_i and q_i in the relations (24) and (25).

It is indicated that, when the hardening arises, the increasing of the stress level reduces the critical void ratio e_{crt} and increases the parameter a. Both changes increase the density function I_e and then limit the developing of hardening. Conversely, when the softening occurs, I_e will decrease to restrict softening and liquefaction. Due to the regulatory function of I_e, the model (21) can describe the shear softening and the residual strength of very loose

Table 1 Material constants for the model (21) in the simulation of the experiments in [46]

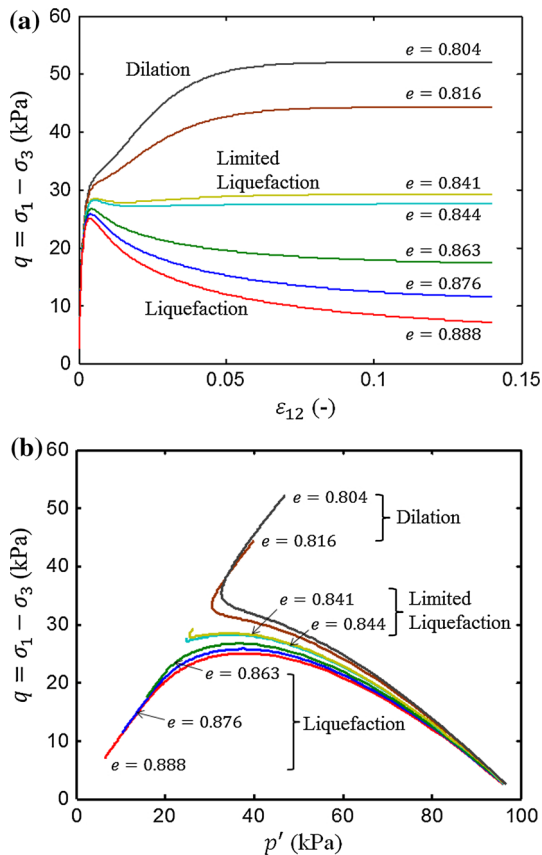| c_1 [–]	c_2 [–]	c_3 [–]	c_4 [–]
−50.0	−629.6	−629.6	1220.8

Fig. 4 Simulation results of (21) for saturated sand with different initial void ratio in undrained simple shear tests: **a** shear strain versus shear stress, **b** mean principal stress versus shear stress

Table 2 Parameters for e_{crt} and a in the simulation of the experiments in [46]

p_1 [–]	p_2 [–]	p_3 [kPa^{-1}]	q_1 [–]	q_2 [–]	q_3 [kPa^{-1}]
0.53	0.45	−0.0018	1.0	−0.4	−0.0001

granular materials. It can be used as the static portion of the new model for debris materials. As shown in Fig. 5, the normal stresses $\sigma_{ii}(i = 1, 2, 3)$ of the very loose specimen with $e = 0.876$ tend to be isotropic when the shear strain is large enough, no matter what is the initial stress state. The isotropic normal stress in the large deformation stage corresponds to the former mentioned thermodynamic pressure P_0.
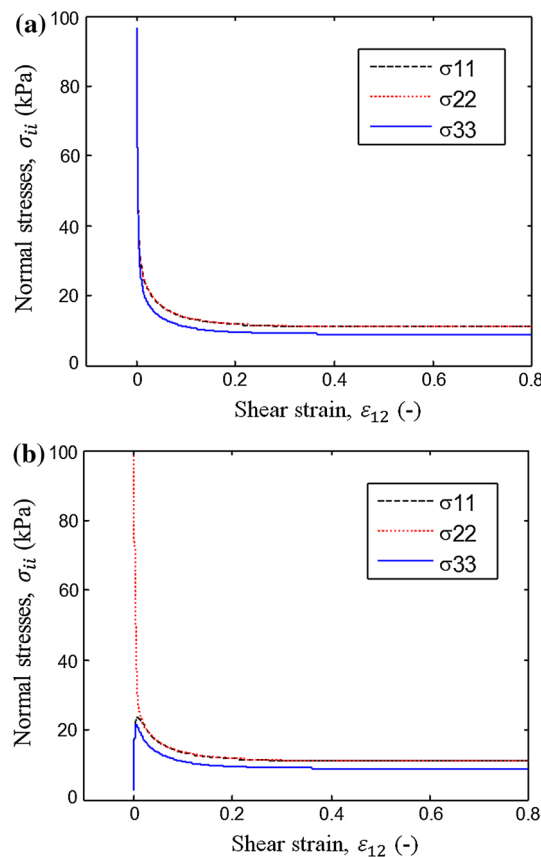

Fig. 5 Normal stresses of the specimens with $e = 0.876$ in the undrained simple shear tests with different initial stress state: **a** $\sigma_{11} = \sigma_{22} = \sigma_{33} = 100$ kPa, **b** $\sigma_{22} = 100$ kPa and $\sigma_{11} = \sigma_{33} = 1$ kPa

4 A new constitutive model for debris materials

Based on the above analysis, the hypoplastic model (21) and the tensor form of the modified Bagnold's model are employed as the static and dynamic portions of the new constitutive model, respectively. The structure of the new model is proposed as

$$\mathbf{T} = \mathbf{T}_h + \mathbf{T}_d. \tag{27}$$

In our former work about the constitutive model of granular-fluid flows [15], the three-dimensional form of the dynamic portion was obtained based on a simplest model structure for describing non-Newtonian fluid (see, for example, [38]). The general three-dimensional form of the dynamic portion is

$$\mathbf{T}_d = -\frac{4K_2}{\tan \alpha_i} \mid II_{D^*} \mid \mathbf{1} + \left(2K_1 + 4K_2 \sqrt{\mid II_{D^*} \mid}\right)\mathbf{D}^* \tag{28}$$

where

$$\mathbf{D}^* = \mathbf{D} - \frac{\text{tr}(\mathbf{D})}{3}\mathbf{1} \tag{29}$$
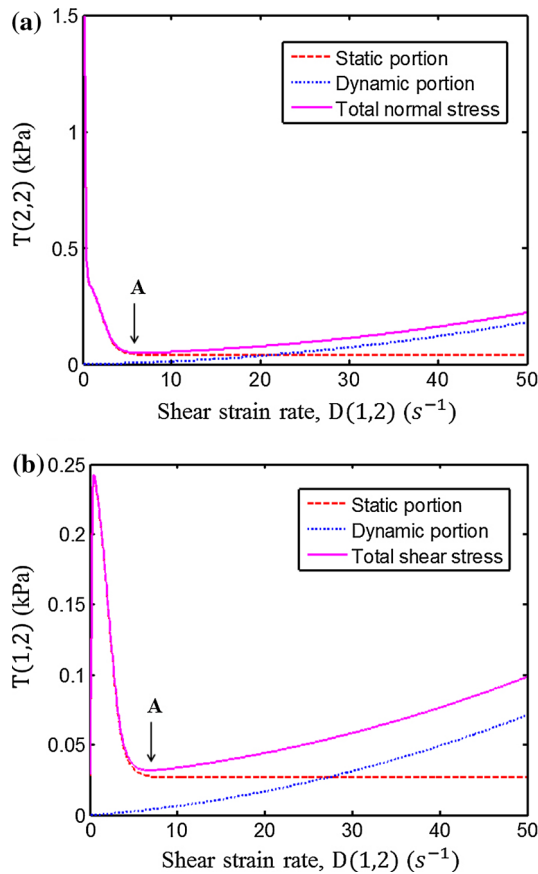
(a)

(b)

Fig. 6 Schematics of the new model (32): **a** shear rate versus normal stress, **b** shear rate versus shear stress

is the strain rate deviator tensor and

$$II_D^* = \frac{1}{2}((\mathrm{tr}\mathbf{D}^*)^2 - \mathbf{tr}(\mathbf{D}^{*2})) \qquad (30)$$

is the second invariant of $\mathbf{D}^*$. It can be easily shown that for a simple shear flow where the strain rate tensor takes the form

$$\mathbf{D} = \begin{bmatrix} 0 & \frac{1}{2}\frac{dU}{dy} & 0 \\ \frac{1}{2}\frac{dU}{dy} & 0 & 0 \\ 0 & 0 & 0 \end{bmatrix} \qquad (31)$$

the dynamic stress (28) is reducible to the dynamic portion of the framework (1).

From (27), the concrete model for debris materials is determined as

$$\mathbf{T} = \int \dot{\mathbf{T}}_h dt - \frac{4K_2}{\tan \alpha_i} \mid II_{D^*} \mid \mathbf{1} + \left(2K_1 + 4K_2\sqrt{\mid II_{D^*} \mid}\right)\mathbf{D}^* \qquad (32)$$

where $\dot{\mathbf{T}}_h$ can be determined by (21).

The structure of the new model is demonstrated by simulating an undrained simple shearing flow. As shown in Fig. 6, a static portion obtained by the hypoplastic model (21) is combined with a dynamic portion to get the total effective stress.

What need to be mentioned is that the static portion, $\mathbf{T}_h$, is rate independent. It is varying due to the accumulation of the shear strain rather than the changing of the shear rate. By merging with the dynamic portion, the total effective stress (32) becomes rate dependent. As shown in Fig. 5, the normal stresses reach a residual constant when the shear strain is approximately 0.4. This process is finished with very small shear velocity in the so-called quasi-static stage. Thus, in the simulation, the shear rate must be kept at a small value before the failure of the granular-fluid mixture to make sure that the static portion is the dominant part in the total effective stress $\mathbf{T}$. The static portion should be much greater than the dynamic portion at the point A in Fig. 6. One approach to meet this requirement in numerical calculations is using small shear strain acceleration and increasing the time steps for the stage before failure.

It is worth mentioning that Wu [42] developed a rate form framework by combining a hypoplastic model and a rate-dependent dynamic model as

$$\mathring{\mathbf{T}} = \mathring{\mathbf{T}}_h(\mathbf{T}_h, \mathbf{D}) + \mathring{\mathbf{T}}_d(\mathbf{D}, \mathring{\mathbf{D}}). \qquad (33)$$

where $\mathring{\mathbf{T}}$ is the total Jaumann stress rate tensor and $\mathring{\mathbf{T}}_d$ is the dynamic part of the Jaumann stress rate tensor. The models developed within this framework may have the capability to account for the different behaviors for loading and unloading. However, the Jaumann strain acceleration tensor, $\mathring{\mathbf{D}}$, makes the implementation of these models in some numerical methods more difficult. It will be an interesting exploration to solve this problem in our future work.

5 Performance of the proposed model

In this section, the new model, (32), will be used to predict the stress–strain relations of granular-fluid flows with different materials and experimental apparatus in some element tests. The experimental data of two annular shear tests as undrained simple shear tests are employed to verify the applicability of the new model. In our former work [15], these two experiments are also simulated by a constitutive model which cannot capture the shear softening of granular-fluid materials in the quasi-static stage. The former simulation results can be used as a control group to highlight the function of the hypoplastic portion in the new model.

Table 3 Parameters for the static portion in the simulation of dry granular flows

c_1 [–]	c_2 [–]	c_3 [–]	c_4 [–]	e_{min} [–]	p_1 [–]	p_2 [–]	p_3 [kPa^{-1}]	q_1 [–]	q_2 [–]	q_3 [kPa^{-1}]
−50	−746.55	−746.55	1855.13	0.563	0.65	0.55	−0.11	1.0	−0.24	−0.013

Table 4 Parameters for the dynamic portion in the simulation of dry granular flows

d [mm]	C_∞ [–]	C_c [–]	ρ_s [kg/m^3]	μ [Pa·s]	$\tan\alpha_i$ [–]
1.0	0.64	0.62	1095	1.83×10^{-5}	$0.40 \sim 0.51$

5.1 Dry granular materials

The experimental data of dry granular materials sheared in a annular shear cell were reported by Savage and Sayed [33]. The data for 1.0 mm spherical polystyrene beads are selected for the element tests. The loads applied by the upper disk range from 100 to 1500 N/m² which is normal to the flow surface. By checking the measured normal stress for 1.0 mm beads, we assume that the initial confining pressure of an element at the upper surface of the specimen has a value around 500 N/m². The exact value of C_∞ was not reported in the literature [33] and here is assumed equal to 0.64 which is a typical value for monosized spheres [2, 16]. Thus, the corresponding minimum void ratio
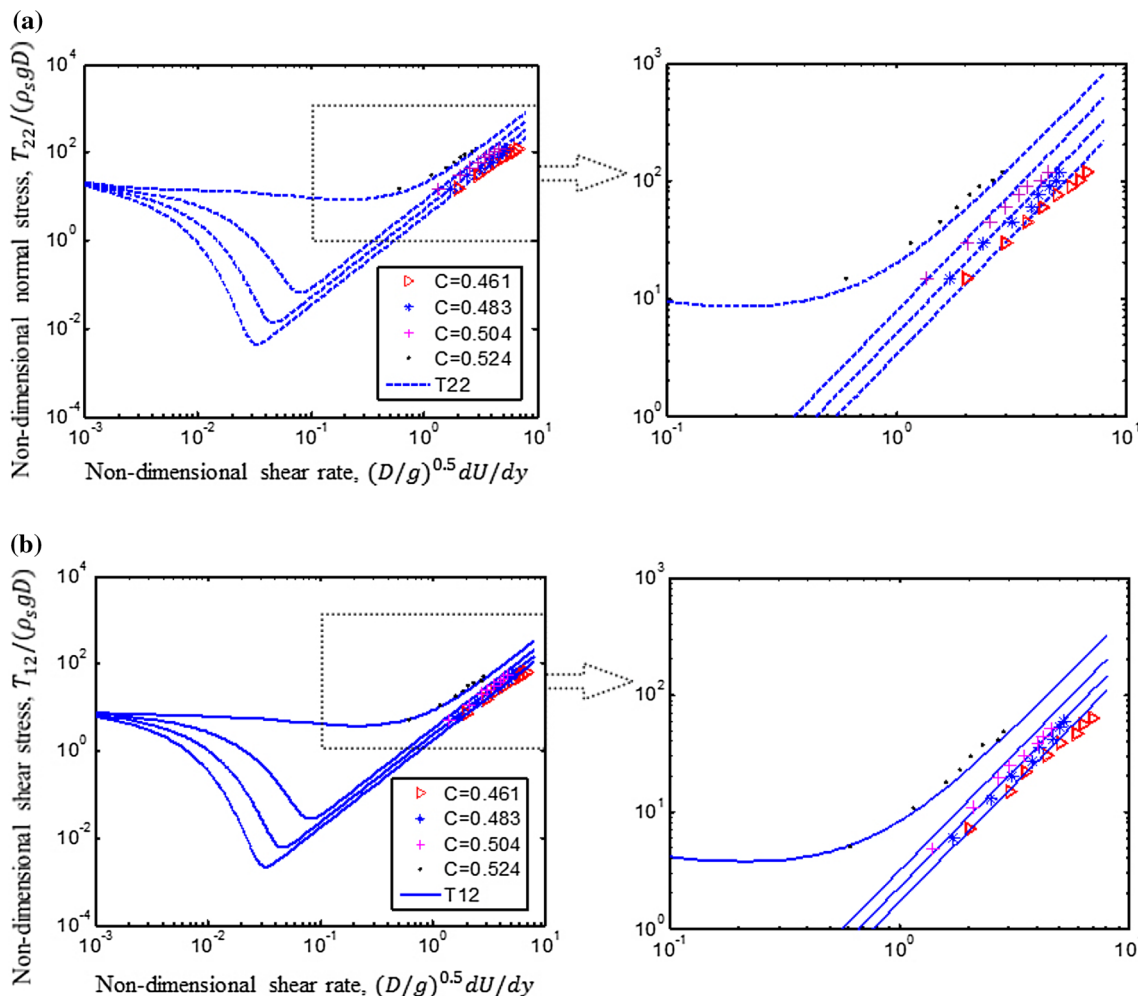
$$e_{min} = \frac{1 - C_\infty}{C_\infty} \tag{34}$$

Fig. 7 Element test results for the dry granular flow with different grain linear concentration: **a** shear rate versus normal stress, **b** shear rate vs shear stress. The experimental data are indicated by various symbols. The *dashed lines* denote the normal stresses while the *solid lines* for the shear stresses

Table 5 Stress state in quasi-static stage calculated by hypoplastic model

Solid volume fraction, C [–]	0.461	0.483	0.504	0.524
Initial void ratio, e [–]	1.17	1.07	0.98	0.91
P_0[Pa]	0	0	0	81
T_0[Pa]	0	0	0	36

Table 7 Parameters for the dynamic portion in the simulation of granular-fluid flows

d [mm]	C_∞ [–]	C_c [–]	ρ_s [kg/m³]	μ [Pa · s]	$\tan\alpha_i$ [–]
1.85	0.61	0.52	2780	1.0×10^{-3}	0.59

is determined equal to 0.563. The critical volume fraction C_c is approximately 0.62 [34]. The internal friction angle ϕ_0 of 1.0 mm spherical beads is 23° and the initial tangent modulus E_i is assumed equal to 15 MPa as a typical value of loose granular materials with the confining pressure is 100 kPa. Based on the identification of parameters introduced in Sect. 3, the material constants $c_1 \sim c_4$ and the parameters for the density function I_e are determined and listed in Table 3.

The parameters for the dynamic portion are listed in Table 4.

As shown in Fig. 7, the predicted results are in good agreement with the experimental data of different solid volume fractions when some typical values are employed for the unstated parameters. The non-quadratic dependence between the stresses and strain rate in the slow shear stage for the samples with $C = 0.524$ is captured by the new model. In the experiments [33], the shear velocity was adjusted to keep the height constant, thereby keeping the volume of the samples unchanged. It is equivalent to the undrained condition in the tests of saturated granular materials. The mean effective stress would decrease from the initial confining pressure to a residual value or zero to offset the tendency of volume compression in the quasi-static stage of very loose granular-fluid mixture. The residual normal and shear stresses, corresponding to the stresses P_0 and T_0 in the framework (1), are determined by the hypoplastic portion and presented in Table 5. Only the test with $C = 0.524$ demonstrates residual strength. It is consistent with the experimental observation [46] that granular materials will be fully liquefied when the initial void ratio exceeds a threshold value. For the looser specimens where $C = 0.504$, 0.483 and 0.461, the stress–strain rate curves in the rapid shear stage show a slope of about 2 in the logarithmic coordinates. It means the linear term T_v which characterizes the effect of the interstitial fluid is insignificant while the quadratic law T_i is dominant in this case as analyzed in the Sect. 2. It proves that the proposed model (32) can describe the shear softening of dry granular materials in the quasi-static stage and the stress–shear rate relation throughout the shear process from the quasi-static stage to the fast shearing stage.

5.2 Granular-water mixture

For the case of a granular-fluid mixture, we take Hanes and Inman's experiments [16] about spherical particles sheared in water as an example. The data for particles with diameter 1.85 mm which were stated as good quality ones are chosen to verify the new model. The maximum measured volume fraction for 1.85 mm particles was reported to be 0.55. Thus, the asymptotic limit C_∞ is presumed to be approximately 0.61 and the minimum void ratio is 0.64. The critical volume fraction is assumed to be 0.52 since partial shearing was observed in the test of the specimen with $C = 0.53$. The load from the upper disk is almost 500 N/m². The internal friction angle ϕ_0 is stated to be 28° and the initial tangent modulus E_i is 15 MPa. The determined material constants $c_1 \sim c_4$ and the parameters for the density function I_e are presented in Table 6.

The parameters of the dynamic portion are listed in Table 7.

The simulation results are shown in Fig. 8. The stress states of the two specimens are reproduced based on the prediction of the residual stresses. The specific values are presented in Table 8. The sample with $C = 0.51$ results in residual strength after failure in the undrained simple shearing. The shear stress–shear rate curves of $C = 0.49$ has a slope less than 2 in the stage with shear rate between 1 and 10 in the logarithmic coordinates. Comparing to the dry granular flows, the effect of the interstitial fluid in a granular-fluid flow is non-negligible. The slight difference between the slopes of predicted curves and the experimental data for $C = 0.49$ in the rapid shear stage implies a nonzero residual strength of this specimen. It may be attributed to that the employed parameters for the hypoplastic portion are not reasonable for this case.

Table 6 Parameters for the static portion in the simulation of granular-fluid flows

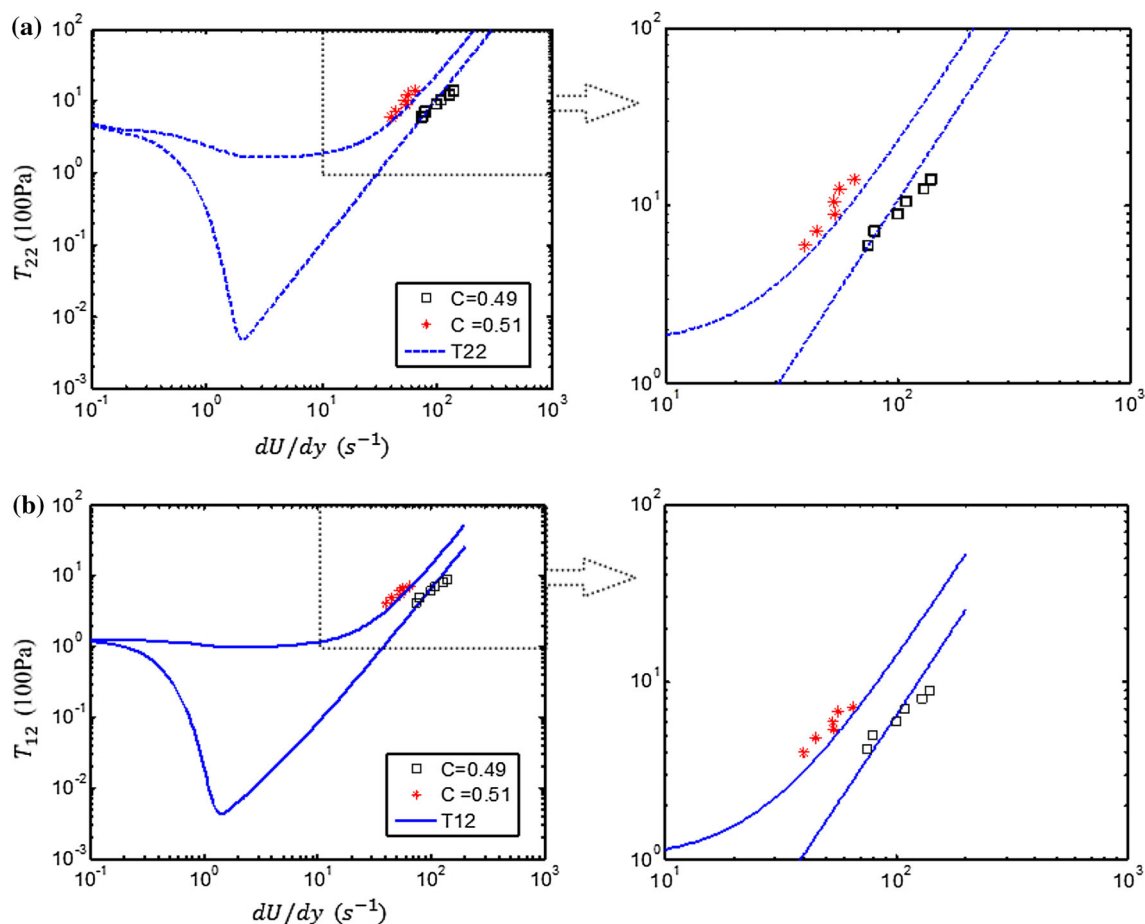| c_1 [–]	c_2 [–]	c_3 [–]	c_4 [–]	$e_{\min}$ [–]	p_1 [–]	p_2 [–]	p_3 [kPa^{-1}]	q_1 [–]	q_2 [–]	q_3 [kPa^{-1}]
−50	−511.31	−511.31	680.53	0.64	0.65	0.55	−0.11	1.0	−0.12	−0.013

Fig. 8 Element test results for the granular-water flows with different solid volume fraction: **a** shear rate versus normal stress, **b** shear rate vs shear stress. The experimental data are indicated by various symbols. The *solid lines* denote the shear stresses and the *dashed lines* are the normal stresses

6 Conclusions

In the initiation of debris flows, the development of excess pore water pressure is considered as the most significant triggering factor. Debris materials are normally simplified as granular-fluid mixture for constitutive modeling. Therefore, a theory which can be used to describe the solid-like behavior of debris materials should have the ability to capture the changing of pore water pressure. Moreover, a constitutive relation for the debris materials in the flowing stage should be rate dependent, in which some important material parameters in a granular-fluid flow, such as solid volume fraction, fluid viscosity and particle density, are taken into account. In a former developed framework [15], a static portion for the friction component and a dynamic portion for the viscous component are combined. The dynamic portion is composed of a linear term for drag force of the fluid and a quadratic term for the collisional force. For a dry granular flow on an inclined plane, the linear term is negligible since

the viscous effect of air is insignificant compare to the frictional and collisional effect of particles. In this case, the model predicts a steady uniform flow over a slope range, which is consistent with the experimental observation [3]. The constitutive relations based on this framework can describe the stress state throughout the shear process from yielding to high-speed shearing. Moreover, a smooth transition is obtained between the so-called macro-viscous and grain-inertia regimes. The applicability of hypoplastic model in describing debris flows before failure is studied by simulating the undrained simple shear test of saturated granular material. Such test condition is particularly relevant to the initiation mechanism of debris flow. Three types of stress–strain behavior in which the 'liquefaction' is regarded as the main factor of debris flow mobilization are reproduced by the hypoplastic model. It is shown that the hypoplastic model has the capability to describe the changes of pore water pressure and further capture the shear softening and hardening behavior of granular-fluid mixtures. Therefore, it

Table 8 Stress state in quasi-static stage calculated by hypoplastic model

Solid volume fraction, C [–]	0.49	0.51
Initial void ratio, e [–]	1.04	0.96
P_0[Pa]	0	173
T_0[Pa]	0	102

is chosen as the static portion of the new model for debris flows. Then, this static part is combined with the tensor form of the modified Bagnold's dynamic model to obtain a new complete model for the modeling of debris materials from static to dynamic state. The new model is employed to simulate two annular shear tests with dry and water-saturated granular materials. In the case of dry granular flow with constant volume, the hypoplastic portion predicts that only the densest one of the four specimens has residual strength. It implies a non-quadratic dependence between the stresses and the shear rate in the slow flowing stage which was observed in the experiments. Similar conclusion is also obtained in the case of water-saturated granular flow. Comparing to the dry granular flow, the linear term T_v, which characterizes the effect of the interstitial fluid, is non-negligible in the granular-fluid flow. The element test results show that the new model is applicable to the modeling of granular materials with different interstitial fluid. The predicted stress–strain curves agree well with the experimental data.

Further verification is still needed for the new model. It is our intention to implement this model in some numerical codes for large deformation, such as SPH and computational fluid dynamics (CFD) codes, to simulate granular-fluid flows in an inclined channel or a rotating drum. As mentioned before, a hypoplastic model developed by Wang and Wu [39] has been implemented in SPH for large deformation analysis [29]. Therefore, SPH will be the preferred choice for further verification of the new model. As mentioned before, the models in the rate form may have the capability to account for the different behaviors for loading and unloading. It will be an interesting exploration to develop the rate form expression for the dynamic portion in which the loading and unloading process can be distinguished.

Compliance with ethical standards

Conflict of interest The authors declare that they have no conflict of interest.

References

1. Bagnold RA (1954) Experiments on a gravity-free dispersion of large solid spheres in a Newtonian fluid under shear. Proc R Soc Lond A Math Phys Sci 225:49–63
2. Bagnold RA (1956) The flow of cohesionless grains in fluids. Proc R Soc Lond A 249:235–297
3. Bailard JA (1978) An experimental study of granular fluid flow. Ph.D. thesis. University of California, San Diego
4. Bailard JA, Inman DL (1979) A reexamination of Bagnold's granular-fluid model and bed load transport equation. J Geophys Res 84:7827–7833
5. Bauer E (1992) Mechanical behavior of granular materials with special reference to oedometric loading. Publication Series of the Institute of Soil Mechanics and Rock Mechanics, Kaflsruhe University. No. 130
6. Bingham EC (1922) Fluidity and plasticity. McGraw-Hill, New York
7. Castro G (1969) Liquefaction of sands. Ph.D. Thesis, Harvard University, Cambridge
8. Chang CS, Hicher P-Y (2005) An elasto-plastic model for granular materials with microstructural consideration. Int J Sol Struct 42:4258–4277
9. Cowin SC (1974) Constitutive relations that imply a generalized Mohr–Coulomb criterion. Acta Mech 20:41–46
10. Fang C, Wu W (2014) On the weak turbulent motions of an isothermal dry granular dense flow with incompressible grains: Part I. Equilibrium turbulent closure models. Acta Geotech 9:725–737
11. Fang C, Wu W (2014) On the weak turbulent motions of an isothermal dry granular dense flow with incompressible grains: part II. Complete closure models and numerical simulations. Acta Geotech 9:739–752
12. Grabe J, Heins E (2016) Coupled deformation seepage analysis of dynamic capacity tests on open-ended piles in saturated sand. Acta Geotech. doi:10.1007/s11440-016-0442-z
13. Gudehus G (1996) A comprehensive constitutive equation for granular materials. Soils Found 36(1):1–12
14. Guo X, Wu W (2015) Some ideas on constitutive modeling of debris materials. In: Wu W (ed) Recent advances in modeling landslides and debris flows. Springer, Vienna, pp 1–9
15. Guo X, Wu W, Wang Y, Peng C (2016) A new constitutive model for granular-fluid flows. Granular Matter. (Under review)
16. Hanes DM, Inman DL (1985) Observations of rapidly flowing granular-fluid materials. J Fluid Mech 150:357–380
17. Hutter K, Svendsen B, Rickenmann D (1996) Debris flow modeling: a review. Contin Mech Thermodyn 8:1–35
18. Iverson RM (2003) The debris-flow rheology myth. In: 3rd International Conference on Debris-Flow Hazards Mitigation: Mechanics, Prediction, and Assessment, Davos. 1, pp. 303–314
19. Iverson RM, Reid ME, LaHusen RG (1997) Debris-flow mobilization from landslides. Annu Rev.Earth Planet Sci 25:85–138
20. Janbu N (1963) Soil compressibility as determined by oedometer and triaxial test. In: Proceedings of the European conference on soil mechanics and foundation engineering, Wiesbaden, Germany. 1, pp. 19–25

21. Jenkins ST, Savage SB (1983) A theory for the rapid flow of identical, smooth, nearly elastic spherical particles. J Fluid Mech 130:187–202

22. Klubertanz G, Laloui L, Vulliet L (2009) Identification of mechanisms for landslide type initiation of debris flows. Eng Geol 109:114–123

23. Li Z, Kotronis P, Escoffier S, Tamagnini C (2016) A hypoplastic macroelement for single vertical piles in sand subject to three-dimensional loading conditions. Acta Geotech 11:373–390

24. Major JJ, Pierson TC (1992) Debris flow rheology: experimental analysis of fine-grained slurries. Water Resour Res 28(3):841–857

25. McTigue DF (1979) A nonlinear continuum model for flowing granular materials. Ph.D. thesis. Stanford University, Stanford, California

26. Mctigue DF, Savage SB (1981) Comment on 'A reexamination of Bagnold's granular-fluid model and bed load transport equation' by J. A. Bailard and D. L. Inman. J Geophys Res 86:4311–4313

27. Nemat-Nasser S (2000) A micromechanically-based constitutive model for frictional deformation of granular materials. J Mech Phys Sol 48:1541–1563

28. Niemunis A, Herle I (1997) Hypoplastic model for cohesionless soils with elastic strain range. Mech Cohes Frict Mater 2:279–299

29. Peng C, Wu W, Yu H, Wang C (2015) A SPH approach for large deformation analysis with hypoplastic constitutive model. Acta Geotech 10:703–717

30. Pouliquen O, Forterre Y (2002) Friction law for dense granular flows: application to the motion of a mass down a rough inclined plane. J Fluid Mech 453:133–151

31. Savage SB (1979) Gravity flow of cohesionless granular materials in chutes and channels. J Fluid Mech 92:53–96

32. Savage SB, Babaei MH, Dabros T (2014) Modeling gravitational collapse of rectangular granular piles in air and water. Mech Res Commun 56:1–10

33. Savage SB, Sayed M (1984) Stresses developed by dry cohesionless granular materials sheared in an annular shear cell. J Fluid Mech 142:391–430

34. Shibata M, Mei CC (1986) Slow parallel flows of a water-granular mixture under gravity, Part I: continuum modeling. Acta Mech 63:179–193

35. Stutz H, Mašín D, Wuttke F (2016) Enhancement of a hypoplastic model for granular soil structure interface behaviour. Acta Geotech. doi:10.1007/s11440-016-0440-1

36. von Soos P (1990) Properties of soil and rock (in German). In: Grundbau taschenbuch part 4, 4th edn, Ernst & Sohn, Berlin

37. von Wolffersdorf PA (1996) Hypoplastic relation for granular materials with a predefined limit state surface. Mech Cohes Frict Mater 1(3):251–271

38. Wang Y, Hutter K (2001) Granular material theories revisited. In: Balmforth NJ, Provenzale A (eds) Geomorphological fluid mechanics. Springer, Berlin, pp 79–107

39. Wang X, Wu W (2011) An update hypoplastic constitutive model, its implementation and application. In: Wan R, Alsaleh M, Labuz J (eds) Bifurcations, instabilities and degradations in geomaterials. Springer, Berlin, pp 133–143

40. Wieczorek GF (1987) Effect of rainfall intensity and duration on debris flows in the central Santa Cruz Mountains, California. In: Costa JE, Wieczorek GF (eds) Debris flows/avalanches: process, recognition, and mitigation. Geological Society of America, Colorado, pp 93–104

41. Wu W, Bauer E, Kolymbas D (1996) Hypoplastic constitutive model with critical state for granular materials. Mech Mater 23:45–69

42. Wu W (2006) On high-order hypoplastic models for granular materials. J Eng Math 56:23–34

43. Wu W, Bauer E (1994) A simple hypoplastic constitutive model for sand. Int J Numer Anal Methods Geomech 18:833–862

44. Wu W, Kolymbas D (2000) Hypoplastic then and now. In: Kolymbas D (ed) Constitutive modelling of granular material. Springer, Berlin, pp 57–105

45. Yang F-L, Hunt ML (2006) Dynamics of particle-particle collisions in a viscous liquid. Phys Fluids 18:121506

46. Yoshimine M, Ishihara K, Vargas W (1998) Effects of principal stress direction and intermediate principal stress on undrained shear behavior of sand. Soils Found 38(3):179–188

47. Yoshimine M, Ishihara K (1998) Flow potential of sand during liquefaction. Soils Found 38(3):189–198